

Elliptic flow, eccentricity and eccentricity fluctuations

Constantin LOIZIDES⁴ for the PHOBOS collaboration

B.Alver⁴, B.B.Back¹, M.D.Baker², M.Ballintijn⁴, D.S.Barton², R.R.Betts⁶, R.Bindel⁷, W.Busza⁴, Z.Chai², V.Chetluru⁶, E.García⁶, T.Gburek³, K.Gulbrandsen⁴, J.Hamblen⁸, I.Harnarine⁶, C.Henderson⁴, D.J.Hofman⁶, R.S.Hollis⁶, R.Hołyński³, B.Holzman², A.Iordanova⁶, J.L.Kane⁴, P.Kulinich⁴, C.M.Kuo⁵, W.Li⁴, W.T.Lin⁵, S.Manly⁸, A.C.Mignerey⁷, R.Nouicer², A.Olszewski³, R.Pak², C.Reed⁴, E.Richardson⁷, C.Roland⁴, G.Roland⁴, J.Sagerer⁶, I.Sedykh², C.E.Smith⁶, M.A.Stankiewicz², P.Steinberg², G.S.F.Stephans⁴, A.Sukhanov², A.Szostak², M.B.Tonjes⁷, A.Trzuppek³, G.J.van Nieuwenhuizen⁴, S.S.Vaurnovich⁴, R.Verdier⁴, G.I.Verés⁴, P.Walters⁸, E.Wenger⁴, D.Willhelm⁷, F.L.H.Wolfs⁸, B.Wosiek³, K.Woźniak³, S.Wyngaardt², B.Wysłouch⁴

¹ Argonne National Laboratory, Argonne, IL 60439-4843, USA

² Brookhaven National Laboratory, Upton, NY 11973-5000, USA

³ Institute of Nuclear Physics PAN, Kraków, Poland

⁴ Massachusetts Institute of Technology, Cambridge, MA 02139-4307, USA

⁵ National Central University, Chung-Li, Taiwan

⁶ University of Illinois at Chicago, Chicago, IL 60607-7059, USA

⁷ University of Maryland, College Park, MD 20742, USA

⁸ University of Rochester, Rochester, NY 14627, USA

(Received December 13, 2006)

Differential studies of elliptic flow are one of the most powerful tools in studying the initial conditions and dynamical evolution of heavy ion collisions. The comparison of data from Cu+Cu and Au+Au collisions taken with the PHOBOS experiment at RHIC provides new information on the interplay between initial geometry and initial particle density in determining the observed final state flow pattern. Studies from PHOBOS point to the importance of fluctuations in the initial state geometry for understanding the Cu+Cu data. We relate the elliptic flow data to the results of our model studies on initial state geometry fluctuations and discuss how we will perform measurements of event-by-event fluctuations in elliptic flow in Au+Au collisions.

Keywords: Participant eccentricity, event-by-event

I. ELLIPTIC FLOW

Studies of the elliptic flow of produced particles via measurements of their azimuthal distribution are important probes of the dynamics of heavy ion collisions. In the collision of two nuclei with finite impact parameter, the almond-shaped overlap region has an azimuthal spatial asymmetry. The asymmetrical shape of the source region can only be reflected in the azimuthal distribution of detected particles if the particles significantly interact after their initial production. Thus, observation of azimuthal anisotropy in the outgoing particles is direct evidence of interactions between the produced particles. In addition, these interactions must occur at relatively early times, since expansion of the source—even if uniform—would gradually erase the magnitude of the spatial asymmetry. Typically, hydrodynamical models are used to quantitatively relate a specific initial source shape and the distribution of emitted particles [1]. At top RHIC energy, $\sqrt{s_{NN}} = 200$ GeV, the elliptic flow signal at midrapidity in Au+Au collisions is described under the assumption of a boost-invariant relativistic hydrodynamic fluid, indicating that there is early equilibration in the colliding system [2].

The azimuthal anisotropy of the initial collision region can be characterized by the eccentricity (ϵ) of the overlap region of the colliding nuclei in the transverse plane. The strength of the elliptic flow, v_2 , is commonly defined by the coefficient of the second harmonic in the Fourier expansion of the azimuthal

particle distribution relative to the reaction plane, Ψ_R , such that $v_2 = \langle \cos(2\phi - 2\Psi_R) \rangle$ [3].

Recent hydrodynamical calculations [4] conclude that v_2 scales approximately with ϵ for small ϵ . Such calculations typically use smooth, event-averaged initial conditions, for which the initial azimuthal asymmetry is well described by the “standard” eccentricity, $\epsilon_{std} = \frac{\sigma_y^2 - \sigma_x^2}{\sigma_x^2 + \sigma_y^2}$, where σ_x^2 (σ_y^2) is the variance of the participant nucleon distribution projected on the x (y) axis, taken to be along (perpendicular to) the impact parameter direction.

PHOBOS has measured elliptic flow as a function of pseudorapidity, centrality, transverse momentum, center-of-mass energy [5–7] and, recently, nuclear species [8]. In particular, the measurements of elliptic flow as a function of centrality provide information on how the azimuthal anisotropy of the initial collision region drives the azimuthal anisotropy in particle production. In fig. 1a, we show the centrality dependence of v_2 at mid-rapidity ($|\eta| < 1$) for Cu+Cu and Au+Au at $\sqrt{s_{NN}} = 62.4$ and 200 GeV collision energies, as obtained from our hit-based analysis method [6, 8]. A substantial flow signal is measured in Cu+Cu at both energies, even for the most central events. This is quite surprising, as according to the initial anisotropy given by ϵ_{std} one expects that v_2 should approach zero as the collisions become more central, similar to what has been found for the Au+Au case.

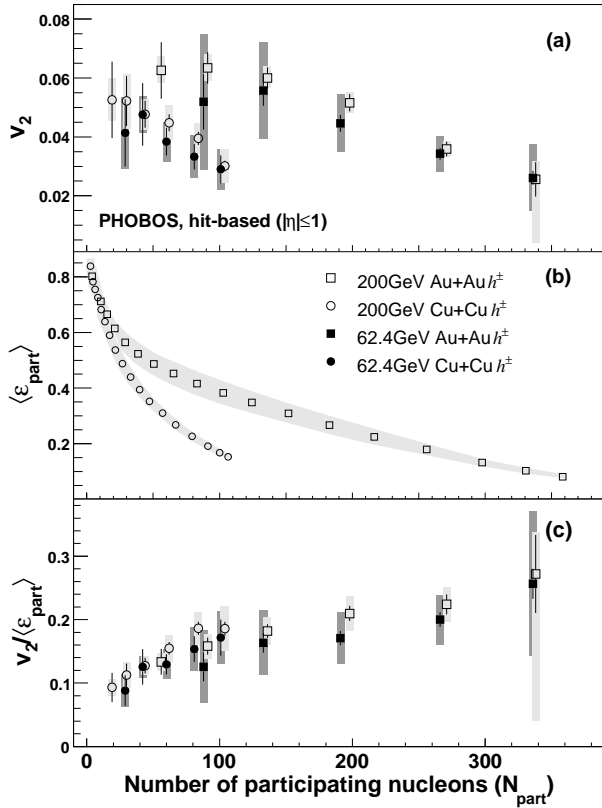


FIG. 1: (a) v_2 (unscaled), (b) $\langle \epsilon_{part} \rangle$ and (c) $v_2/\langle \epsilon_{part} \rangle$ vs. N_{part} for Cu+Cu and Au+Au collisions at $\sqrt{s_{NN}} = 62.4$ and 200 GeV. 1- σ statistical errors (bars) and 90% C.L. systematic errors (bands) are shown. Data points and eccentricity calculation are from Refs. [6, 8].

II. ECCENTRICITY FLUCTUATIONS

As a possible explanation for the large v_2 signal in the small Cu+Cu system, we have argued that event-by-event fluctuations in the shape of the initial collision region may drive the elliptic flow [8, 9]. For small systems or small transverse overlap regions, fluctuations in the nucleon positions frequently create a situation where the minor axis of the overlap ellipse is not aligned with the impact parameter vector. These fluctuations are neglected in the definition of ϵ_{std} . Instead, we have introduced the ‘‘participant eccentricity’’,

$$\epsilon_{part} = \frac{\sqrt{(\sigma_y^2 - \sigma_x^2)^2 + 4\sigma_{xy}^2}}{\sigma_x^2 + \sigma_y^2}. \quad (1)$$

This definition accounts for the nucleon position fluctuations by quantifying the eccentricity event-by-event with respect to the minor axis of the overlap ellipse, in the frame, defined by Ψ_{part} , that diagonalizes the ellipse. Note, $\sigma_{xy} = \langle xy \rangle - \langle x \rangle \langle y \rangle$, σ_x^2 and σ_y^2 are the (co-)variances of the x and y participant nucleon position distributions expressed in the original frame, given by Ψ_R . For a system with a large number of nucleons, the covariance term is comparatively small. Therefore, the average values of ϵ_{std} and ϵ_{part} over many events are similar for all, but the most peripheral interactions for the Au+Au system. For the smaller Cu+Cu system, however, fluctuations in

the nucleon positions become more important for all centralities [8].

In fig. 1b, we show a Glauber model calculation of ϵ_{part} as a function of N_{part} for Cu+Cu and Au+Au. The colliding nuclei are built by randomly placing nucleons according to a Woods-Saxon distribution. Excluded volume effects are addressed by requiring a minimum inter-nucleon separation distance of 0.4 fm. As opposed to ϵ_{std} , where averages are implicitly over participants and events, the variance expressions in ϵ_{part} are averaged event-by-event over participants, individually. To check how the event-by-event interpretation of the Glauber calculation depends on the external parameter settings, we varied a number of sources of systematic error, like the nuclear radius, nuclear skin depth, nucleon-nucleon inelastic cross-section σ_{NN} and minimum nucleon separation. Varying each specific parameter within reasonable limits, the individual contributions were added in quadrature to determine the 90% confidence level errors shown in fig. 1b.

In order to compare the elliptic flow signals across nuclear species and with hydrodynamical predictions, it is important to scale out the difference in the initial asymmetry of the collision geometry. In fig. 1c, we show the eccentricity-scaled flow for Cu+Cu and Au+Au, $v_2/\langle \epsilon_{part} \rangle$, as a function of centrality. The scaled data are very similar for both the Cu+Cu and Au+Au collision systems at the same number of participants. It is important to note that the apparent scaling does not rely on the fine-tuning of the Glauber parameter settings, as is evident from the systematic errors, which are rather small (see fig. 1b).

III. ELLIPTIC FLOW FLUCTUATIONS

If the proposed participant fluctuations are driving the value of v_2 event-by-event, as suggested by our $\langle v_2 \rangle$ analysis, then we expect them to contribute to event-by-event elliptic flow fluctuations. As mentioned above, ideal hydrodynamics leads to $v_2 \propto \epsilon$ [4]. Assuming the same relation holds event-by-event, this would imply that $\sigma_{v_2}/\langle v_2 \rangle = \sigma_\epsilon/\langle \epsilon \rangle$, where σ_{v_2} (σ_ϵ) is the standard deviation of the event-by-event distribution of v_2 (ϵ). Using our $\langle v_2 \rangle$ data (fig. 1a) and the Monte Carlo Glauber simulation to obtain σ_ϵ (and $\langle \epsilon \rangle$) for the participant eccentricity, we estimate σ_{v_2} to be about 2% for all centralities, except the most central Au+Au collisions at $\sqrt{s_{NN}} = 200$ GeV. This estimate leads to rather large relative fluctuations ($\sigma_{v_2}/\langle v_2 \rangle$) between 35 and 50%. It is important to note that these estimates neglect other sources of elliptic flow fluctuations.

In the following, we will give a brief overview of the analysis method that we have developed to measure flow fluctuations with PHOBOS in peripheral and semi-central Au+Au collisions. Details can be found in Ref. [10]. We seek to discriminate known (statistical) from unknown (presumably dynamical) contributions to observed flow fluctuations. Ideally, they would add according to $\sigma_{v_2,obs}^2 = \sigma_{v_2,dyn}^2 + \sigma_{v_2,stat}^2$. This relation holds if the average of the measurement, $\langle v_2^{obs} \rangle$, gives the true average in the data, $\langle v_2 \rangle$, and if the resolution of our method is independent of the true value. Neither of these conditions are fully satisfied in the event-by-event mea-

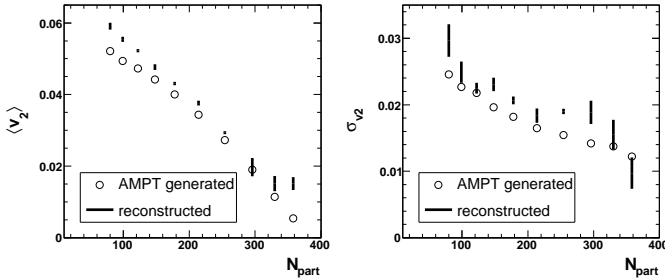


FIG. 2: Generated and reconstructed $\langle v_2 \rangle$ (left) and σ_{v_2} for AMPT vs. N_{part} . The generated signal is extracted from a mixed-event analysis based on the true Monte Carlo particle information. The reconstructed signal is averaged over results of running the complete flow fluctuation analysis in 10 vertex bins using the kernel created from the modified HIJING samples. The black lines represent the $\pm 1\sigma$ error on the mean, with the mean centered (not shown).

surement of v_2 . Therefore, a more detailed knowledge of the response function is required. We define $K(v_2^{\text{obs}}, v_2, n)$ as the distribution of the event-by-event observed elliptic flow, v_2^{obs} , for events with constant input flow value, v_2 , and multiplicity, n . Assuming a set of events has an input v_2 distribution given by $f(v_2)$, then $g(v_2^{\text{obs}})$, the distribution of v_2^{obs} , will be given according to

$$g(v_2^{\text{obs}}) = \int_0^\infty K(v_2^{\text{obs}}, v_2, n) f(v_2) N(n) dv_2 dn, \quad (2)$$

where $N(n)$ is the multiplicity distribution of the events in the given set of events (centrality bin). Thus, our event-by-event elliptic flow fluctuation analysis consists of three steps:

- Finding the observed v_2 distribution, $g(v_2^{\text{obs}})$, for a set of events by an event-by-event measurement of v_2^{obs} .
- Construction of the kernel, $K(v_2^{\text{obs}}, v_2, n)$, by studying the detector response for sets of constant (known) input value of v_2 and multiplicity n .
- Calculating the true v_2 distribution, $f(v_2)$, by finding a solution to eq. (2).

For the event-by-event measurement we use a maximum likelihood method, making use of all hit information from the multiplicity array to measure a single value, v_2^{obs} , while allowing an efficient correction for the non-uniformities in the acceptance. We model the measured pseudorapidity dependence of v_2 according to $v_2(\eta) = v_2 \cdot (1 - |\eta|/6)$, with

$v_2 \equiv v_2(0)$, which is known to describe our mean v_2 data reasonable well. We define the probability distribution function (PDF) of a particle to be emitted in the direction (η, ϕ) for an event with v_2 and reaction plane angle ϕ_0 as $P(\eta, \phi | v_2, \phi_0) = p(\eta)[1 + 2v_2(\eta) \cos(2\phi - 2\phi_0)]$. The normalization $p(\eta)$ is constructed such that the PDF, folded with the PHOBOS acceptance, yields the same value for different sets of parameters (v_2, ϕ_0) . Maximizing $\prod_{i=1}^n P(\eta_i, \phi_i | v_2, \phi_0)$ as a function of v_2 and ϕ_0 allows us to measure v_2^{obs} event-by-event. We determine the response function $K(v_2^{\text{obs}}, v_2, n)$ in bins of v_2 and n using modified HIJING events. Flow of constant magnitude (v_2) with a flat reaction plane distribution (ϕ_0) is introduced into generated HIJING Au+Au events. This is achieved by redistributing the resulting particles in each event in ϕ randomly according to $1 + 2v_2(\eta) \cos(2\phi - 2\phi_0)$, using their generated η positions. The modified HIJING events are run through GEANT to obtain the PHOBOS detector response. To finally extract $f(v_2)$, we for now simply assume a Gaussian distribution with $\langle v_2 \rangle$ and σ_{v_2} . For given values of $\langle v_2 \rangle$ and σ_{v_2} , it is possible to take the integral in eq. (2) to obtain the expected distribution, $g_{\text{exp}}(v_2^{\text{obs}} | \langle v_2 \rangle, \sigma_{v_2})$. By comparing the expected and observed distributions, values for $\langle v_2 \rangle$ and σ_{v_2} are obtained from a minimized χ^2 of the data to the expectation. As outlined in Ref. [10], the whole analysis procedure was verified on similar HIJING events as used to construct the kernel, and found to successfully reconstruct the input fluctuations, provided $\langle v_2 \rangle \geq 0.03$.

Here, we report on a study with fully simulated AMPT events in order to verify the analysis with a different type of “data” events than used to create the kernel, since in AMPT flow builds up dynamically. To minimize acceptance effects, the analysis is done in bins of collision vertex. Fig. 2 shows the averaged results obtained from the different vertex bins compared to the generated signal. Since the information about the generated v_2 in AMPT has not been readily available on an event-by-event basis, we extracted the generated $\langle v_2 \rangle$ and σ_{v_2} from a mixed-event analysis based on the true Monte Carlo particle information. We conclude that the developed analysis chain is able to reconstruct the fluctuations to a satisfactory degree over a large range in centrality, in samples of “data” that are different from the ones used to construct the kernel.

This work was partially supported by U.S. DOE grants DE-AC02-98CH10886, DE-FG02-93ER40802, DE-FC02-94ER40818, DE-FG02-94ER40865, DE-FG02-99ER41099, and W-31-109-ENG-38, by U.S. NSF grants 9603486, 0072204, and 0245011, by Polish KBN grant 1-P03B-062-27(2004-2007), by NSC of Taiwan Contract NSC 89-2112-M-008-024, and by Hungarian OTKA grant (F 049823).

[1] P. F. Kolb *et al.* PLB **500**, 232 (2001).
 [2] B. B. Back *et al.* [PHOBOS], NPA **757**, 28 (2005).
 [3] A.M. Poskanzer and S.A. Voloshin, PRC **58**, 1671 (1998).
 [4] R. S. Bhalerao *et al.*, PLB **627**, 49 (2005).
 [5] B. B. Back *et al.* [PHOBOS], PRL **89**, 222301 (2002).

[6] B. B. Back *et al.* [PHOBOS], PRL **95**, 122303 (2005).
 [7] B.B. Back *et al.* [PHOBOS], PRC **72**, 051901(R) (2005).
 [8] B. Alver *et al.* [PHOBOS], arXiv:nucl-ex/0610037.
 [9] S. Manly *et al.* [PHOBOS], arXiv:nucl-ex/0510031.
 [10] B. Alver *et al.* [PHOBOS], arXiv:nucl-ex/0608025.